Supplementary Information (SI) for Physical Chemistry Chemical Physics.

Supporting Information: Crystal-Field Tuning of Valley-Related Multiple Hall Effects in Ferromagnetic Monolayers

Xinyang Li[1,2], and Liang Ma[1,2*]
[1]Key Laboratory of Quantum Materials and Devices of Ministry of Education, School of Physics, Southeast University, Nanjing 211189, China
[2]Suzhou Laboratory, Suzhou 215004, China
* Corresponding authors
liang.ma@seu.edu.cn

Electronic Support Information

Part I : Structure of ScX and TiY monolayer and Phonon spectra of single-layer.

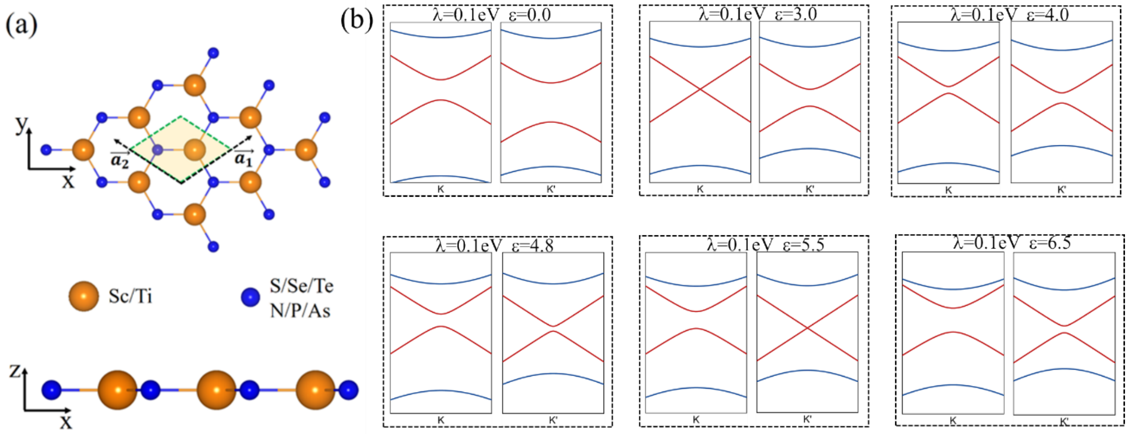

Fig.S1. (a) Top and side views of the lattice structure for ScX (X =S, Se, Te) and TiY(Y=N, P, As) monolayer with lattice vectors $\vec{a}_1$ and $\vec{a}_2$. The Sc,Ti and X, Y atoms are depicted by the orange and blue balls, respectively. The rhombus covered with light orange shadow denotes the unit cell. (b) Evolution of the band structures around the K and K' valleys under different SOC strengths λ and biaxial strains ε. Blue and red lines represent spin-up and spin-down bands, respectively.

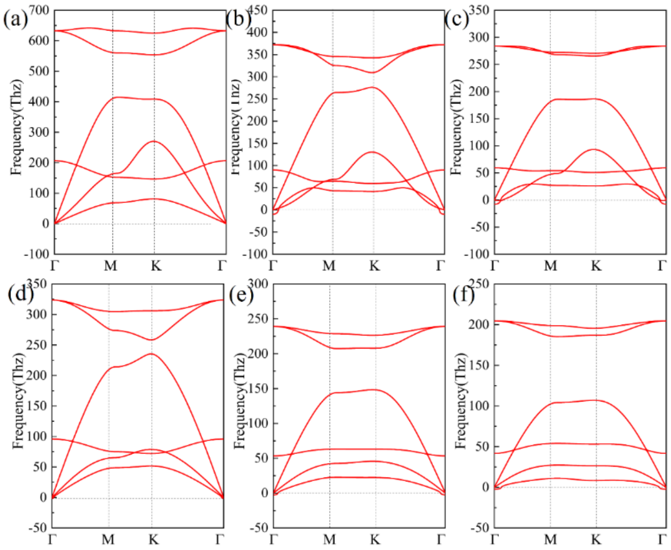

Fig.S2. [(a)–(f)] The calculated phonon dispersion curves along the high-symmetry lines within the first BZ of the (a) TiN, (b) TiP, (c) TiAs, (d) ScS, (e) ScSe, (f)ScTe, respectively.

The AIMD simulations at 300 K show that the total energies of the ScX and TiY monolayers fluctuate around equilibrium values during the simulation, and the final atomic configurations remain intact without structural collapse or bond breaking, confirming their thermal stability.

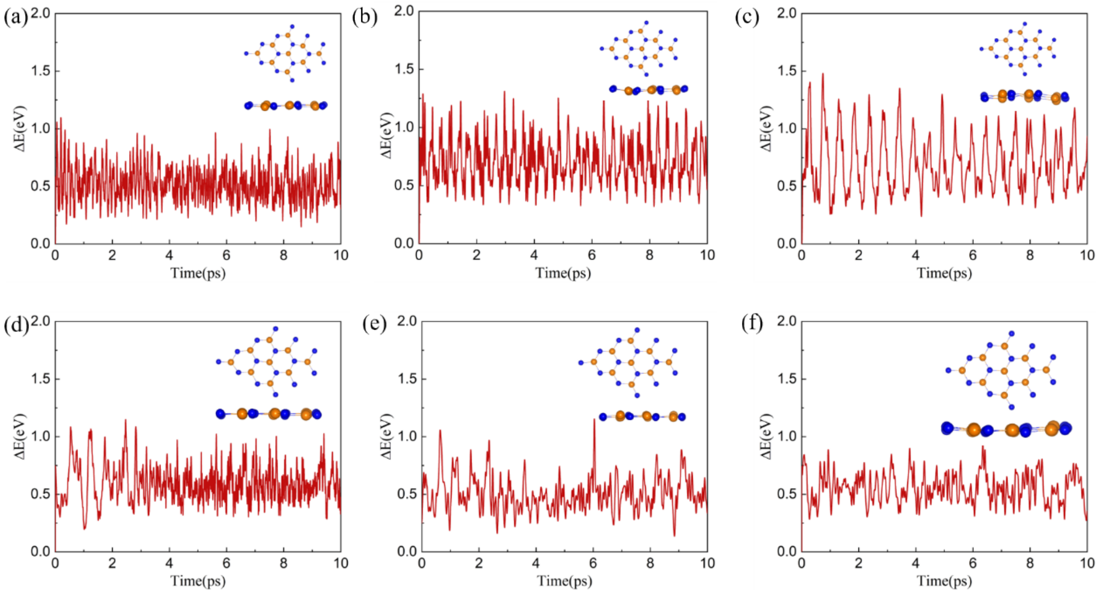

Fig.S3. AIMD simulation results for ScX and TiY monolayers at 300 K. The time-dependent total energy fluctuations and the final atomic configurations are shown for (a) TiN, (b) TiP, (c) TiAs, (d) ScS, (e) ScSe, and (f) ScTe, respectively. The total energies fluctuate around equilibrium values during the simulations, and the final structures remain intact without structural collapse or bond breaking, indicating the thermal stability of these monolayers.

The calculated formation energies of TiN, TiP, TiAs, ScS, ScSe, and ScTe are −2.3, −1.9, −1.7, −3.2, −2.5, and −2.7 eV, respectively, indicating that these monolayers are energetically favorable.

	TiN	TiP	TiAs	ScS	ScSe	ScTe
E_{form}(eV)	-2.3	-1.9	-1.7	-3.2	-2.5	-2.7

Table S1: Calculated formation energies E_{form} of ScX and TiY monolayers. The negative formation energies indicate that these monolayers are energetically favorable with respect to the corresponding elemental reference phases.

Part II: The parameters of model.

	Δ	m_c	m_v	D	λ	$\hbar v_F$
(eV)	0.94	0.5	0.7	8.0	0.2	1.30

Table S2: The parameters used in the model, the parameters obtained through fitting to the bands from first-principles calculations.

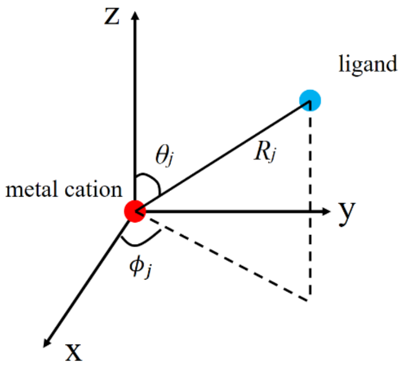

Fig.S4. Diagram of the metal cation and its j-th ligand.

Part III: **Monte Carlo simulations for magnetic transition temperatures**

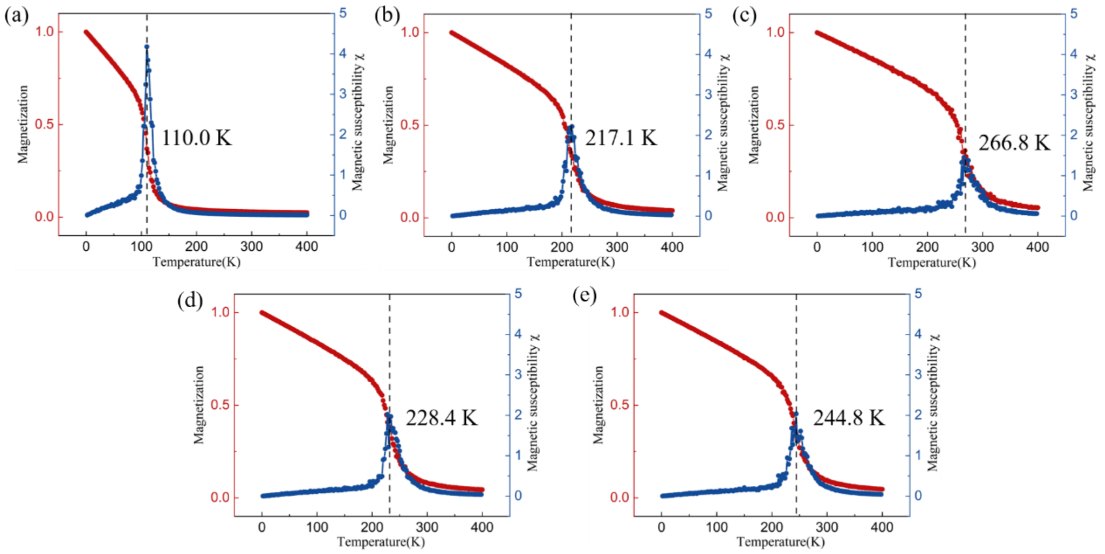

Fig.S5. Temperature-dependent magnetization and magnetic susceptibility of ScX and TiY monolayers obtained from classical Monte Carlo simulations. The results are shown for (a) TiN, (b) TiP, (c) ScS, (d) ScSe, and (e) ScTe, respectively.

Part IV: **electron localization function (ELF) of ML ScS.**

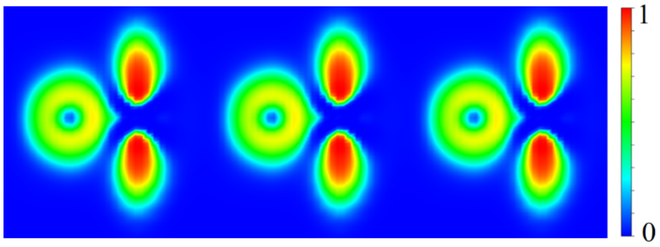

Fig.S6. Electron localization function (ELF) of ML ScS.

The ELF distribution shows that the electrons are mainly localized around the S atoms, while the electron localization in the Sc–S bond region is relatively weak, indicating that the Sc–S bonding is predominantly ionic with a weak covalent component.

Part V: **Band structures of *monolayers.***

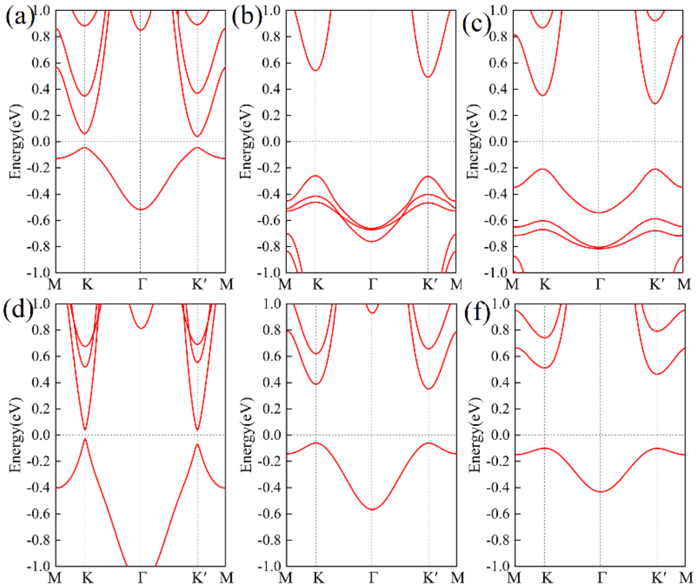

Fig.S7. Band structures along the high-symmetry lines within the first BZ of the ML (a)TiN, (b)TiP, (c)TiAs, (d)ScS, (e)ScSe, (f)ScTe, respectively.

Part VI: **Band structures of ML-ScS.**

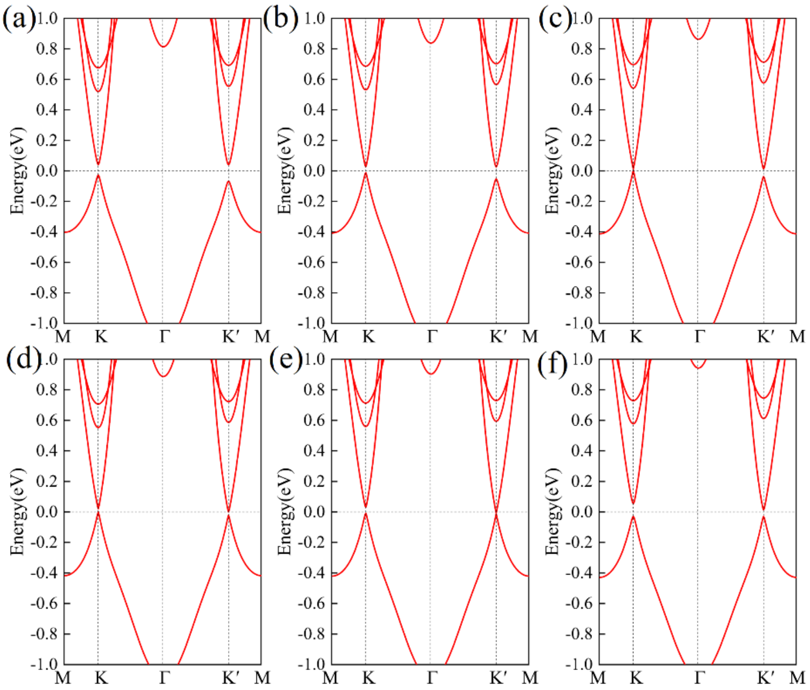

Fig.S8. Band structures of ML ScS with SOC under strain of (a)0%, (b) 0.3%, (c)0.7%, (d) 0.9%, (e) 1.1% and (f) 1.6%. The Fermi level is set to 0 eV.

Part VII: **Band structures of ML-ScS calculated by HSE06.**

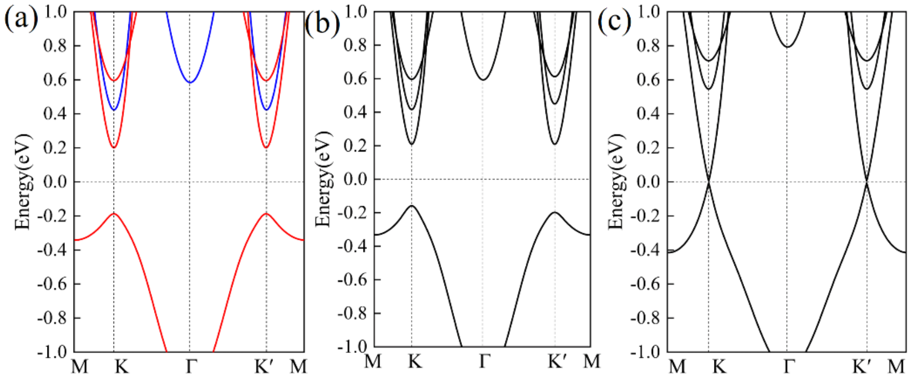

Fig.S9. Band structures of ML ScS calculated by HSE06 with spin-polarization (a) and SOC (b) and under strain of (c)2.3%

Part VIII: Anomalous Hall conductivity vs chemical potential for ML ScS.

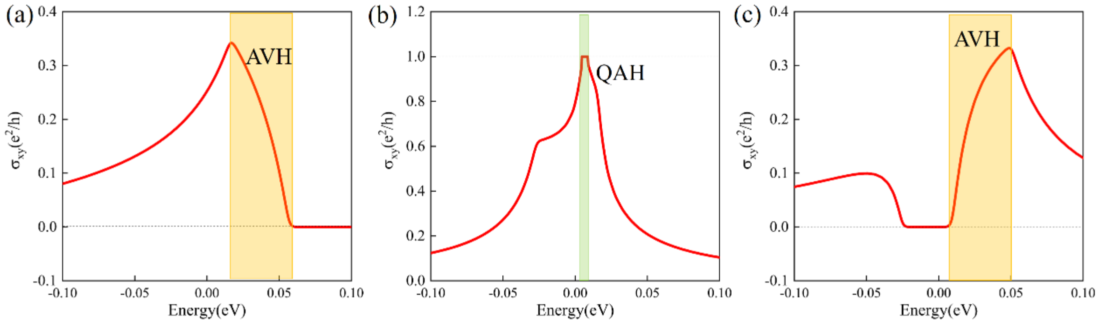

Fig.S10. Anomalous Hall conductivity vs chemical potential for ML ScS under strain of (a)0.0 %, (b) 0.9%, (c)1.6%.

Part IX: Computational methods and details.

All structural and electronic properties are calculated by using Vienna ab initio simulation package based on spin-polarized density functional theory (DFT). The exchange correlation potential is described with the Perdew-Burke-Ernzerhof (PBE) of the generalized gradient approximation (GGA). In the PBE+U calculations, the rotationally invariant Dudarev approach was adopted to describe the localized 3d electrons of the transition-metal atoms. The effective Hubbard parameters were set to U_{eff}=2.5eV for Sc-3d orbitals and U_{eff}=2.0eV for Ti-3d orbitals. The projected argument wave (PAW) potential is used to describe the ion-electron potential. The energy cutoff of the plane wave is 500 *eV*. The Brillouin zone uses a convergent 11×11×1 k mesh for structural relaxation and 33×33×1 for electronic analysis. For the MAE calculations, a denser 51×51×1 k-point mesh was used to ensure numerical accuracy. Both the atomic position and the lattice constant are relaxed until the force and energy converge to 0.001*eV*/Å and 10^{-7} *eV*/atom. For XY, in order to avoid the interaction between adjacent layers, a vacuum space of about 20Å is applied along the c direction. Based on the density of functional perturbation theory, the Phonon dispersion spectrum of XY was calculated with the PHONOPY program, and in this process, we use a 3×3×1 supercell. Ab initio molecular dynamics (AIMD) simulations are performed with a 3×3×1 supercell at 300 K with a total simulation time of 10 ps. The topological features of edge states were calculated by means of maximally localized Wannier functions implemented in the WANNIER90 package.